BOULDER DISTRIBUTIONS AROUND YOUNG LUNAR IMPACT CRATERS: CASE STUDY OF SOUTH RAY CRATER. R. N. Watkins[1], K. Mistick[2], B. L. Jolliff[2], S. J. Lawrence[3], [1]Planetary Science Institute, 1700 E. Fort Lowell, Suite 106, Tucson, AZ 85719, rclegg-watkins@psi.edu , [2]Washington University in St. Louis, Saint Louis, MO 63130, [3]Johnson Space Center, Houston, TX.

Introduction: Understanding the distributions of boulders around young lunar craters is essential for determining how far craters distribute boulders, how these distributions change over time, and for selecting safe landing sites for future missions. High-resolution (0.5-2 m/pixel) Lunar Reconnaissance Orbiter Camera (LROC) Narrow Angle Camera (NAC) images [1] provide one of the best tools for counting and measuring boulders on the lunar surface, down to the meter scale. Here, we describe how to calculate and use several types of boulder distributions, using an LROC NAC count of boulders around South Ray crater. Ultimately these distributions can be compared across craters of various ages to constrain the rate at which rocks become regolith [2-5], and across craters of various sizes to determine the maximum distance to which craters distribute boulders [6]. Variations in these distributions can also be related to properties such as crater size, age, depth-to-diameter ratios, regolith thickness, and terrain type [5-7].

South Ray is a 700 m, 2 Ma-old [8] crater located in the Descartes Highlands, near the Apollo 16 landing site (9.15° S, 15.38° E). South Ray is young relative to the estimated time required to break down boulders [2,4], so most of its boulders are still present on the surface. Our count for South Ray, shown in **Fig. 1**, only includes boulders in the southern portion because the northern half is likely contaminated with boulders from nearby North Ray crater. We assume the distribution would be the same for the northern portion.

Methods: We use Crater Helper Tools in ArcMap to visually identify and estimate the size of boulders. In NAC images, boulders are positive relief features and appear as bright, sun-facing pixels adjacent to dark, generally elongated shadows in low-sun images. Boulders are measured as ellipses, allowing us to capture both the long and short dimension. Using NAC images with a 0.5-1 m/pixel resolution, the smallest boulders that we identify with confidence are ~1-2 m (>3 pixels including the shadow). We determine the distance of each boulder from the crater center using the haversine formula, and count until it appears that no more boulders originating from the crater are present. We omit boulders inside the rim because steep slopes inside rims refresh the rock population as crater walls degrade.

Boulder Distributions*:* The distributions we investigate with our counts are boulder size-range, size-frequency, and frequency-range distributions. We calculate boulder distances from crater rims in units of crater radii to find how the frequency of boulders varies as a function of distance from the crater, and to enable comparison of distributions around craters of different sizes.

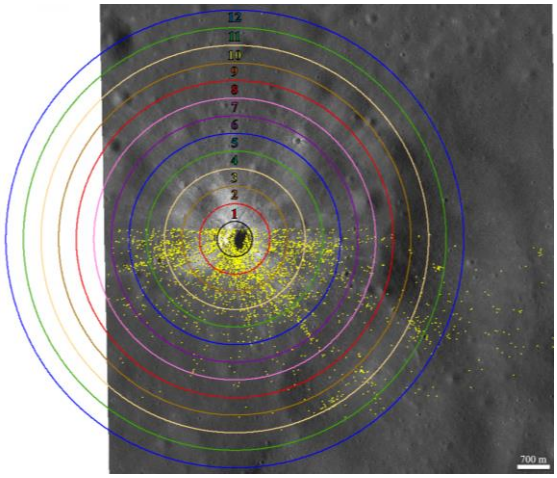

Fig. 1: Boulder counts centered at South Ray crater. Colored circles and numbers indicate distances from the rim (black circle) in crater radii.

Boulder Size-Range Distributions (SRDs) inform how the distribution of boulder sizes varies with distance from the crater. Previous studies have shown that larger boulders occur closer to the crater rim and smaller boulders occur at all distances [6,9-10]. South Ray has boulders present out to ~18 crater radii from the rim, as indicated by its SRD plot (**Fig. 2a**). The largest boulders (>6 m) are found closer to the rim and smaller boulders are found at all distances. Because South Ray is so young, large boulders are still present out to farther distances than for older craters (*e.g.*, Cone [5]), supporting the idea that larger boulders are structurally weaker and degrade more quickly [4,11].

SRDs can be used to constrain the maximum boulder size at any given distance from a crater using quantile regression fits. For example, the 99th quantile of a fit indicates the typical size below which 99% of the boulders fall (at any given radius; **Fig. 2a**). These quantile regression fits use the power-law form $d_{max} = aR^{-b}$, where d_{max} is the maximum boulder diameter at a range R (distance from rim). Performing quantile regressions at multiple craters of different diameters should provide enough regression parameter values (a and b) to allow us to derive equations that predict the maximum boulder size as a function of crater size.

Boulder Size-Frequency Distributions (SFDs) provide information on the quantity of boulders at each observed size distributed around the crater. The most common way to plot SFDs is by plotting the diameter of the boulders against their cumulative frequency per count area (Fig 2b; the roll-off around 2 m is due to the limit of resolution of boulders in the NAC image.). This relationship is fit by a power-law, consistent with fits found

by other studies [2 ,9, 12-14] of the form $y=ax^b$, where y is the cum. freq./km^2 and x is the boulder diameter.

Previous studies have suggested that as crater size increases, both the total number of boulders and the size of the largest boulder ejected increases [9,10,13,15,16]. This trend can be tested by comparing SFDs across craters of various sizes (with similar ages). Our preliminary work counting around craters at legacy landing sites suggests that this trend holds [6,7]; deviations can be attributed to differences in impact velocity, with higher velocity impacts producing more small boulders [16].

Boulder Range-Frequency Distributions (RFDs) are used to assess the areal density (frequency) of boulders per crater radii. RFDs inform the maximum distance that ejecta blocks are transported by impacts of various sizes (which has not been studied until now). At South Ray, we see that the areal density of boulders decreases with increasing distance from the crater rim, as expected (**Fig 2c**. [6]). As with the other distributions, the FRD can be fit by a power law function. Assessing FRDs for craters of various sizes and ages will both inform the maximum distance that craters distribute boulders and how the areal density of boulders changes over time.

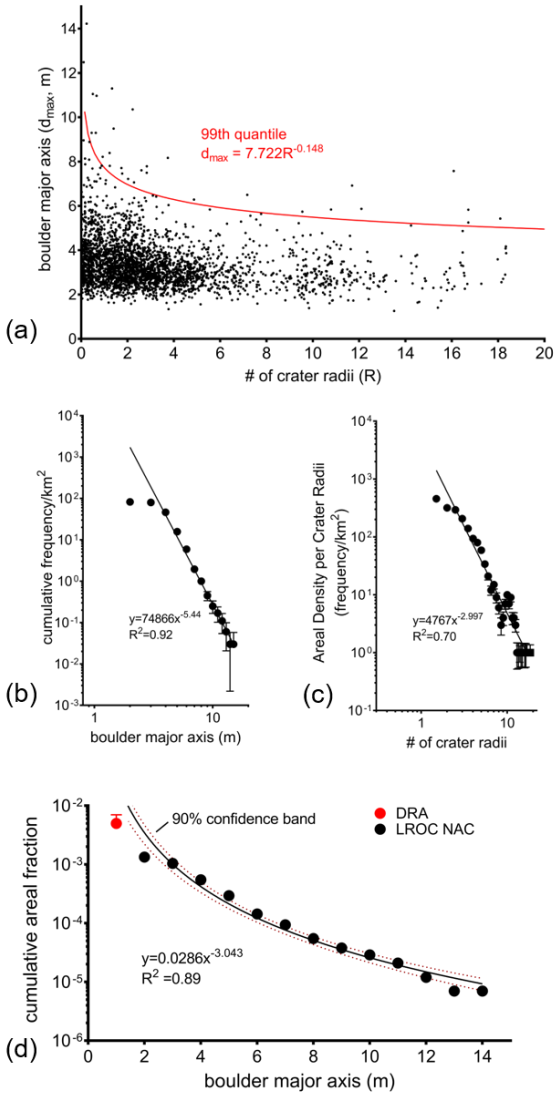

Fig. 2: Boulder distributions at South Ray crater: (a) size-range distribution (red curve is 99th quantile), (b) size-frequency distribution, (c) range-frequency distribution, and (d) cumulative areal fraction.

Diviner Rock Abundance: NAC boulder distributions can be used to validate Diviner rock abundance (DRA) data [6], which provides a measure of the areal density of a surface covered in boulders [14]. To do this, we calculate the cumulative areal fraction (CAF) of the surface covered in boulders by dividing the area of our NAC-measured boulders (binned by size) by the total count area. Previous work found that LROC counts closely predict similar CAF as Diviner [6]. The CAF derived from the count at South Ray (**Fig. 2d**) extrapolates to a value at 1 m slightly higher than the Diviner-estimated RA, but fits within the 90% confidence envelope of the error on the DRA value. The relationship between CAF and boulder size can be used to extrapolate to boulders <1 m to match the sensitivity of Diviner, and to extrapolate to sub-meter boulder populations [17], which is a useful tool for landing site safety analyses.

Conclusions: Boulder distributions are a powerful tool for understanding the rate at which rock becomes regolith and the distance to which craters of different sizes distribute boulders. We have demonstrated, using South Ray as an example, the utility of boulder distributions. Combining SRDs, SFDs, and RFDs across craters of various sizes and ages, as discussed in a companion abstract [7], will allow us to test models of boulder breakdown rates, with long-term implications for understanding the Moon's regolith production rate**.** The ability to predict boulder size distributions as a function of distance from a crater will be particularly useful in informing potential boulder hazards for future missions.

Acknowledgements: This work is supported by the NASA Lunar Data Analysis Program, Grant 80NSSC17K0343.

References: [1] Robinson et al. (2010) *Space Sci. Rev. 150,* 81–124. [2] Basilevsky et al. (2013) *PSS, 89,* 118–126. [3] Basilevsky et al. (2015) *PSS, 117,* 312-328. [4] Ghent et al. (2014) *Geology, 42,* 1059–1062. [5] Mazarouei and Ghent (2017) *48th LPSC,* Abstract #2507. [6] Watkins et al. (2017) *48th LPSC,* Abstract #1245. [7] Watkins et al., *this meeting,* Abstract #1201. [8] Arvidson et al. (1975) *Moon, 13,* 259–276. [9] Bart and Melosh (2010) *Icarus, 209,* 337–357. [10] Krishna and Kumar (2016) *Icarus, 264,* 274-299. [11] Housen and Holsapple (1999) *Icarus, 142,* 21-33. [12] Shoemaker et al. (1969) *Surv. Proj. Final Report II,* 21-136. [13] Cintala and McBride (1995) *NASA TM-104804.* [14] Bandfield et al. (2011) *JGR 116.* [15] Moore (1971) *NASA SP-232,* 26-27. [16] Bart and Melosh (2007) *GRL, 34,* doi:10.1029/2007gl029306. [17] Elder et al. (2016) *AGU Fall Mtg,* Abstract #P24A-04.